JOURNAL OF NEUROTRAUMA 35:1694–1704 (July 15, 2018)

DOI: 10.1089/neu.2017.5275

Transient Receptor Potential Melastatin 4 Induces Astrocyte Swelling But Not Death after Diffuse Traumatic Brain Injury

Karen M. Gorse,[1] Mary Kate Lantzy,[2] Eun D. Lee,[3] and Audrey D. Lafrenaye[1]

Abstract

Traumatic brain injury (TBI) is a prevalent disease with significant costs. Although progress has been made in understanding the complex pathobiology of focal lesions associated with TBI, questions remain regarding the diffuse responses to injury. Expression of the transient receptor potential melastatin 4 (Trpm4) channel is linked to cytotoxic edema during hemorrhagic contusion expansion. However, little is known about Trpm4 following diffuse TBI. To explore Trpm4 expression in diffuse TBI, rats were subjected to a diffuse central fluid percussion injury (CFPI) and survived for 1.5 h to 8 weeks. The total number of Trpm4+ cells, as well as individual cellular intensity/expression of Trpm4, were assessed. Hemotoxylin and eosin (H&E) labeling was performed to evaluate cell damage/death potentially associated with Trpm4 expression following diffuse TBI. Finally, ultrastructural assessments were performed to evaluate the integrity of Trpm4+ cells and the potential for swelling associated with Trpm4 expression. Trpm4 was primarily restricted to astrocytes within the hippocampus and peaked at 6 h post-injury. While the number of Trpm4+ astrocytes returned to sham levels by 8 weeks post-CFPI, cellular intensity occurred in region-specific waves following injury. Correlative H&E assessments demonstrated little evidence of hippocampal damage, suggesting that Trpm4 expression by astrocytes does not precipitate cell death following diffuse TBI. Additionally, ultrastructural assessments showed Trpm4+ astrocytes exhibited twice the soma size compared with Trpm4- astrocytes, indicating that astrocyte swelling is associated with Trpm4 expression. This study provides a foundation for future investigations into the role of Trpm4 in astrocyte swelling and edema following diffuse TBI.

Keywords: astrocyte; cell death; diffuse pathology; traumatic brain injury; Trpm4

Introduction

Traumatic brain injury (TBI) remains one of the leading disorders affecting the United States population, resulting in billions of dollars spent annually and extensive personal and societal consequences associated with persistent morbidity.[1,2] Although our knowledge of the complex pathologies associated with TBI-induced focal lesions has progressed, information regarding the pathological progression following diffuse brain injury remains limited. Understanding the pathogenesis of diffuse injuries following TBI is crucial, as diffuse pathologies are highly correlated to ensuing morbidity.[3–7]

Transient receptor potential melastatin 4 (Trpm4) is a unique member of the transient receptor potential (TRP) family in that it is not permeable to divalent cations, such as Ca^{2+}, as are most of the other TRP family members.[8] Rather, Trpm4 is activated by intracellular Ca^{2+} and is a non-selective monovalent cation channel, which depolarizes the cell membrane and modulates intracellular Ca^{2+} levels in a variety of cell types.[9,10] Unlike all other TRP family members, Trpm4 is inhibited by intracellular adenosine triphosphate (ATP).[11,12] These unique properties have prompted the study of Trpm4 in various cellular processes.

Work focusing on focal brain damage implicated *de novo* expression of Trpm4, as a component of the Sur1–Trpm4 channel, with the progression of cytotoxic edema leading to cell death and hemorrhagic contusion expansion.[13–17] The heteromeric sulfonylurea receptor 1 (Sur1)–Trpm4 channel has similar properties to the homomeric Trpm4 channel, including nonselective permeability to monovalent cations and regulation by Ca^{2+} and ATP; however, Sur1 increases Trpm4's sensitivity to Ca^{2+}. Trpm4-mediated contusion expansion is thought to be triggered by the influx of intracellular Ca^{2+} and decrease in ATP within damaged cells following injury. Higher levels of intracellular Ca^{2+} activate the Trpm4 channel and without ATP present to modulate Trpm4, the channel

[1]Department of Anatomy and Neurobiology, [3]Department of Obstetrics and Gynecology, Virginia Commonwealth University, Richmond, Virginia.
[2]Glen Allen High School, Glen Allen, Virginia.

remains open. Opening of Trpm4 allows indiscriminate influx of monovalent cations, generating an osmotic gradient that leads to cellular water influx and precipitates extreme cell swelling and ultimate cell death via oncosis.[9,10,12,13,16,18,19] Inhibition or reduction of Trpm4 reduces lesion size and cell death and improves behavioral outcome following various injuries.[13,20,21] Additionally, the sulfonylurea class drug glyburide (also known as glibenclamide), which inhibits the Sur1 component of the Sur1–Trpm4 channel, has been shown to reduce hemorrhagic contusion expansion and cell death precipitated by progressive cytotoxic edema in rodents sustaining severe focal TBI.[21–24]

While there is compelling evidence that expression of Trpm4 plays a role in hemorrhagic contusion expansion and cell death in certain brain injury paradigms, there is little knowledge regarding the Trpm4 channel following diffuse TBI. In this study, we began to address this knowledge gap by assessing the expression of Trpm4 following a diffuse central fluid percussion injury (CFPI)[25] in which no hemorrhagic contusions form over an 8-week time course.

Methods

Animals

Experiments were conducted using protocols in accordance with the Virginia Commonwealth University institutional ethical guidelines concerning the care and use of laboratory animals (Institutional Animal Care and Use Committee, Virginia Commonwealth University), which adhere to regulations including but not limited to those set forth in the *Guide for the Care and Use of Laboratory Animals, 8th Edition* (National Research Council). Animals were housed in individual cages on a 12 h light-dark cycle with free access to food and water. Forty-four adult male Sprague-Dawley rats weighing 350–450 g were used for this study. Any animal that lost more than 20% of their pre-injury body weight or precipitated gross brain pathology (contusion, subdural hematoma, or gross tissue loss) was excluded from analysis. No animals met exclusion criteria in this study. Animals were euthanized and histologically evaluated at 1.5 h ($n=2$), 3 h ($n=2$), 6 h ($n=9$), 1 day ($n=7$), 2 days ($n=1$), 1 week ($n=8$), 4 weeks ($n=8$), or 8 weeks ($n=7$) post-injury.

Surgical preparation and injury induction

Animals were anesthetized with 4% isoflurane in 30% O_2 and 70% N_2O then intubated and ventilated with 2% isoflurane in 30% O_2 and 70% N_2O throughout the duration of the surgery. Body temperature was maintained at 37°C with a rectal thermometer connected to a feedback-controlled heating pad (Harvard Apparatus, Holliston, MA). Animals were placed in a stereotaxic frame (David Kopf Instruments, Tujunga, CA). A midline incision was made between bregma and lambda and a 4.8 mm circular craniotomy was made along the sagittal suture midway between bregma and lambda for injury induction. The procedures used to induce CFPI were consistent with those previously described.[4,25] Briefly, a Leur-Loc syringe hub was affixed to the craniotomy site and dental acrylic (methyl-methacrylate; Hygenic Corp., Akron, OH) was applied around the hub and allowed to harden. Animals were removed from the stereotaxic frame and injured at a magnitude of 2.05 ± 0.15 atmospheres. The pressure pulse was measured by a transducer affixed to the injury device and displayed on an oscilloscope (Tektronix, Beaverton, OR). Immediately after the injury, the animal was reconnected to the ventilator and physiologic monitoring device and the hub and dental acrylic were removed *en bloc*. Gelfoam was placed over the craniotomy/injury site and the scalp was sutured. The animals were then allowed to recover and were returned to clean home cages. Identical surgical procedures were followed for sham-injured animals, without release of the pendulum to induce injury.

Tissue processing

At appropriate time-points between 1.5 h and 8 weeks post-injury, the animals were injected with 150 mg/kg euthasol, then underwent transcardial perfusion with 0.9% saline followed by 4% paraformaldehyde/ 0.2% gluteraldehyde in Millonig's buffer (136 mM sodium phosphate monobasic/109 mM sodium hydroxide) for immunohistochemical or electron microscopic (EM) processing and analysis. After transcardial perfusion, the brains were removed, post-fixed for 24 h, then sectioned coronally in 0.1 mol/L phosphate buffer with a vibratome (Leica, Banockburn, IL) at a thickness of 40 μm from bregma to $\sim$4.0 mm posterior to bregma. Sections were collected serially in 12 well-plates and stored in Millonig's buffer at 4°C.

Fluorescent immunohistochemistry

Tissue slices were triple labeled with Trpm4, glial fibrillary acidic protein (GFAP) and ionized calcium binding adaptor molecule 1 (Iba-1). Triple-labeled samples were prepared by blocking tissue in 5% normal horse serum (NHS)/1.5% triton-X for 1 h, then incubating with goat anti Trpm4 (1:200) overnight at 4°C. Tissue was then incubated with donkey anti-goat Alexa 568 (1:700; Cat.# A11057; Life Technologies, Carlsbad, CA). The tissue was then re-blocked with 5% NHS, incubated overnight at 4°C with rabbit anti Iba-1 (1:1500; Cat.# 19-19741; Wako Chemicals, Richmond, VA) and Alexa Fluor 488 conjugated mouse anti GFAP (1:1000; Cat.#MAB3402X; EMD Millipore Corp., Temecula, CA) then incubated with Alexa Fluor 633 conjugated goat anti-rabbit (1:700; Cat.# A21082; Life Technologies). All labeled tissue was mounted using Vectashield hardset mounting medium with 4',6-diamidino-2-phenylindole (Cat. # H-1500; Vector Laboratories, Burlingame, CA).

Assessment of Trpm4 expression and cell surface area via confocal microscopy

To evaluate Trpm4 expression, tissue triple-labeled for Trpm4 (Alexa-568 secondary), GFAP (Alexa-488 secondary), and Iba-1 (Alexa 647 secondary) was visualized on a Zeiss LSM 710 system (Carol Zeiss, Oberkochen, Germany). To determine the total percent of Trpm4+ cells that co-labeled with either GFAP or Iba-1, sequentially scanned confocal micrographs were taken using the 40$\times$ objective (four micrographs/regions of interest [ROIs] for each section; two sections assessed for each animal [sham, $n=4$; 6 h, $n=3$; 1 day, $n=2$; 1 week, $n=3$; 4 weeks, $n=3$; and 8 weeks, $n=3$]). The total number of Trpm4+ cells colocalized with either GFAP or Iba-1 using the colocalization finder plugin for FIJI software (NIH, Bethesda, MD) were counted by eye.

To evaluate the number of Trpm4+ cells, tiled images of the right and left hippocampus from the same sections assessed above (two sections per animal) were generated and the total number of Trpm4+ cells within the hippocampal fissure or gray matter of the hippocampus were counted by two independent investigators using FIJI software (National Institutes of Health, Bethesda, MD). All investigators were blinded to animal group throughout both image acquisition and analysis. The area of the hippocampal fissure and gray matter were calculated using FIJI. Data was expressed as number of Trpm4+ astrocytes/100 μm^2.

For additional assessment of the Trpm4+ population, the same tiled confocal micrographs were used. The background was subtracted and images were thresholded in FIJI to allow individual Trpm4+ cells to be added to the ROI manager for intensity/expression assessment of individual Trpm4+ cells using the original confocal images. Intensity/expression of Trpm4 was assessed using

corrected total cell fluorescence on every individual cell within one systematically random section per animal.[26] The integrated density of each Trpm4+ cell within either the hippocampal fissure or gray matter was calculated and corrected for background labeling, using the following formula: background corrected total cell fluorescence = individual Trpm4+ cell Integrated density-(area of the Trpm4+ cell × average mean gray value of section background). The surface area and the mean gray value of each individual Trpm4+ cell also were assessed in FIJI.

Preparation of tissue for light microscopy

In preparation for light and electron microscopic (EM) analysis, tissue was labeled with goat anti-Trpm4 (1:200; Cat.# sc-27540; Santa Cruz Biotechnology, Inc., Dallas, TX) using heat-induced epitope retrieval. Briefly, tissue slices were placed in 0.1M citrate buffer (pH 6.0) and microwaved at 650 W to a temperature of 45°C. Tissue slices were then blocked with 5% NHS, followed by incubation with biotinylated rabbit anti-goat immunoglobulin G (1:1000; Cat. #BA-5000; Vector Laboratories) secondary antibody. Sections were then incubated in avidin biotinylated enzyme complex using the Vectastain ABC kit (Vector Laboratories) followed by visualization with 0.05% diaminobenzidine/0.01% hydrogen peroxide/ 0.3% imidazole (DAB) in 0.1 M phosphate buffer. The tissue was then either mounted, dehydrated and cover-slipped for light microscopy, or processed for EM analysis. Light micrographs were acquired with a Nikon Eclipse 800 microscope (Nikon, Tokyo, Japan) equipped with an Olympus DP71 camera (Olympus, Center Valley, PA) and qualitatively assessed for Trpm4 expression ($n = 2$ animals for each time-point).

Evaluation of cell damage/death

To evaluate numbers of damaged/dead cells following injury, two sequential randomly selected, sections per animal (sham, $n = 7$; 6 h, $n = 5$; 1 day, $n = 5$; 1 week, $n = 4$; 2 weeks, $n = 4$; 4 weeks, $n = 4$ animals) were stained with H&E and assessed as described previously.[27] Briefly, tissue was mounted on gelatin-coated slides before dehydration and rehydration. Rehydrated tissue was incubated in Gills hematoxylin (Leica Biosystems) followed by bluing agent (Leica Biosystems) and three dips in 0.25% eosin Y/0.005% acetic acid/95% ethanol before sections were cleared through increasing concentrations of ethanol and cover-slipped with Permount (Thermo Fisher Scientific, Waltham, MA). Sections were visualized using a Nikon Eclipse 800 microscope. Assessments were done for both sides of the hippocampus. The number of damaged neurons, delineated by eosinophilic cytoplasm and condensed nuclei, was counted by an investigator blind to the animal group and expressed as the number of damaged cells/100 um^2.

Electron microscopy and ultrastructural analysis

Tissue to be used for EM analysis was labeled against Trpm4 using DAB, as described in the ''Preparation of tissue for light microscopy'' section, osmicated, dehydrated, and embedded in epoxy resin on plastic slides. After resin curing, areas of interest were identified using light microscopy. These areas were removed, mounted on plastic studs, and 70-nm sections were cut and mounted on Formvar-coated slotted grids. The grids were stained in 5% uranyl acetate in 50% methanol and 0.5% lead citrate. Electron micrographs were imaged using a JEOL JEM 1230 transmission electron microscope equipped with Ultrascan 400SP CCD and Orius SC1000 CCD cameras (Gatan, Pleasanton, CA). All electron micrographs were evaluated for ultrastructural pathology consistent with cellular damage, including mitochondrial change, vesicular swelling, pyknosis, or peripheral lucent zones. Electron micrographs of Trpm4+ ($n = 110$) and Trpm4- ($n = 57$) astrocytes also were assessed for soma size with FIJI software using the following formula: soma size = total soma area - area of nucleus.

Statistical analysis

Data were tested for normality prior to utilizing parametric or non-parametric assessments. Animal number for each group was determined by an *a priori* power analysis using effect size and variability previously observed in the lab when assessing pathology between either sham and injured groups ($n \geq 2$ shams at each time-point) or two different injured populations ($n \geq 4$ injured at each time-point) using the CFPI model, an alpha = 0.05, and a power of 80%. One-way analysis of variance (ANOVA) and Bonferroni *post hoc* test were performed for all between group histological analyses. Two-way ANOVA was used to evaluate significant interactions between injury and time. Spearman's rho test was used for correlation assessments. Statistical significance was set to $p < 0.05$. Data are presented as mean ± standard error of the mean.

Results

Trpm4 is expressed in hippocampal astrocytes following diffuse brain injury

To qualitatively assess the potential expression of the Trpm4 channel following diffuse brain injury, we utilized immunohistochemical labeling in coronal brain sections from adult male rats sacrificed at various time-points following CFPI. While labeling against Trpm4 in sham-injured rodents was minimal, Trpm4 was observed as early as 1.5 h post-injury in the white matter of the hippocampal fissure (Fig. 1). Trpm4 labeling in a population of diffusely distributed stellate cells also was observed in the gray matter of the hippocampus by 3 h and was found throughout the hippocampus from 6 h to 8 weeks post-CFPI (Fig. 1C-H).

Since both microglia and astrocytes have a stellate cellular morphology, we sought to elucidate the cell type that expressed Trpm4 following diffuse brain injury. Co-labeling studies were performed against Trpm4 and the astrocyte marker GFAP, as well as the microglial marker Iba-1. While Trpm4 did not co-label with Iba-1 at any time-point post-CFPI, consistent overlap between Trpm4 and GFAP was observed throughout the post-injury time course (percent of Trpm4+ cells that were also GFAP+: sham = 84.32 ± 11.45; 6 h = 94.09 ± 2.19; 1 day = 86.69 ± 9.31; 1 week = 95.21 ± 2.36; 4 weeks = 95.83 ± 4.17; 8 weeks = 94.53 ± 2.40), demonstrating that Trpm4 is expressed in astrocytes following diffuse TBI (Fig. 2).

Trpm4 expression peaks at 6 h following diffuse TBI and occurs in region-specific waves

To quantitatively assess the progression of Trpm4 expression following diffuse TBI, the number of Trpm4+ astrocytes was assessed within either the hippocampal fissure or the gray matter of the hippocampus (Fig. 3A) in sham-injured rats and rats sustaining CFPI and survived for 6 h, 1 day, 1week, 4 weeks, or 8 weeks following TBI. Counts were compared directly with time-point consistent shams. There were significantly more Trpm4+ astrocytes in the hippocampal fissure and hippocampal gray matter 6 h, 1 week, and 4 weeks following CFPI compared with sham controls (one-way ANOVA: 6 h hippocampal fissure, $F_{1,7} = 14.71$, $p = 0.006$; 6 h gray matter, $F_{1,7} = 7.82$, $p = 0.027$; 6 h whole hippocampus, $F_{1,7} = 8.84$, $p = 0.021$; 1 week hippocampal fissure, $F_{1,6} = 6.24$, $p = 0.047$; 1 week gray matter, $F_{1,6} = 18.28$, $p = 0.005$;

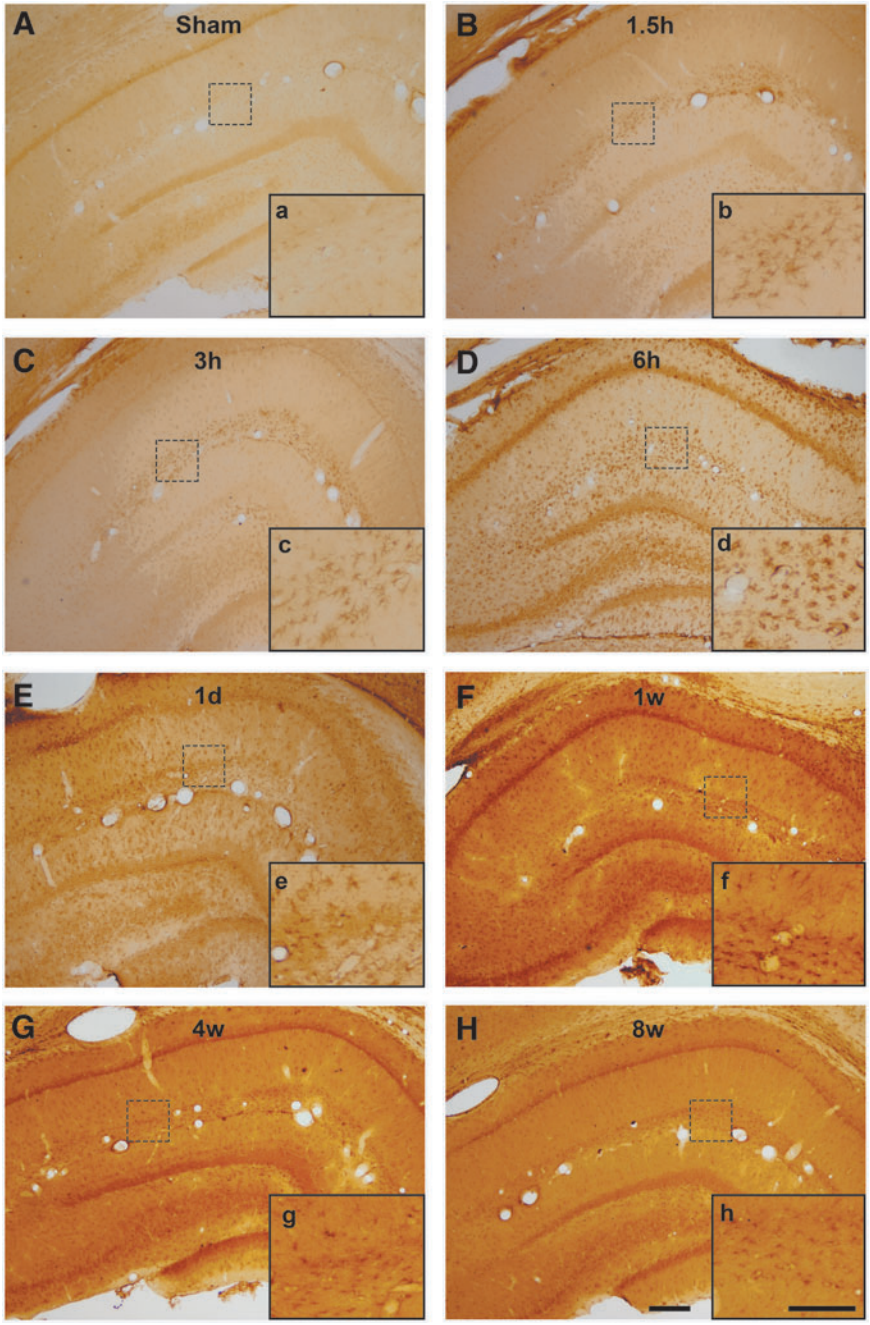

FIG. 1. Transient receptor potential melastatin 4 (Trpm4) is expressed diffusely throughout the hippocampus from 1.5 h to 8 weeks following diffuse traumatic brain injury (TBI). Representative light micrographs of hippocampi from **(A)** sham-injured rats or rats subject to a central fluid percussion injury (CFPI) and killed at **(B)** 1.5 h, **(C)** 3 h, **(D)** 6 h, **(E)** 1 day, **(F)** 1 week, **(G)** 4 weeks or **(H)** 8 weeks post-TBI ($n = 2$ animals/time-point). At 1.5 h post-CFPI expression of Trpm4 is restricted to the white matter of the hippocampal fissure. At 3 h post-injury Trpm4+ cells are observed diffusely distributed throughout the hippocampus; however, the expression within the hippocampal fissure is predominant. Inlaid boxes a, b, c, d, e, f, g, and h are higher magnification micrographs of regions indicated by the dashed squares within (A), (B), (C), (D), (E), (F), (G), and (H). Diffuse expression of Trpm4 throughout the hippocampus persists through 8 weeks post-injury. Scale bar (A), (B), (C), (D), (E), (F), (G), (H): 200 μm. Scale bar a, b, c, d, e, f, g, h: 100 μm.

1 week whole hippocampus, $F_{1,6} = 17.38$, $p = 0.006$; 4 weeks hippocampal fissure, $F_{1,6} = 10.77$, $p = 0.017$; 4 weeks gray matter, $F_{1,6} = 8.77$, $p = 0.025$; 4 weeks whole hippocampus, $F_{1,6} = 9.53$, $p = 0.021$; Fig. 3B-E). While the average number of Trpm4+ hippocampal astrocytes at 1 day post-CFPI was only slightly reduced compared with the number at 6 h, and despite the strong trend toward more Trpm4+ astrocytes at 1 day post-CFPI compared with 1 day shams, this difference was not significant (one-way ANOVA: 1 day hippocampal fissure, $F_{1,4} = 6.34$, $p = 0.066$; 1 day gray matter, $F_{1,4} = 1.01$, $p = 0.373$; 1 day whole hippocampus, $F_{1,4} = 1.52$, $p = 0.285$; Fig. 3C). Additionally, the number of Trpm4+ astrocytes at 8 weeks post-TBI was indistinguishable from 8 weeks sham-

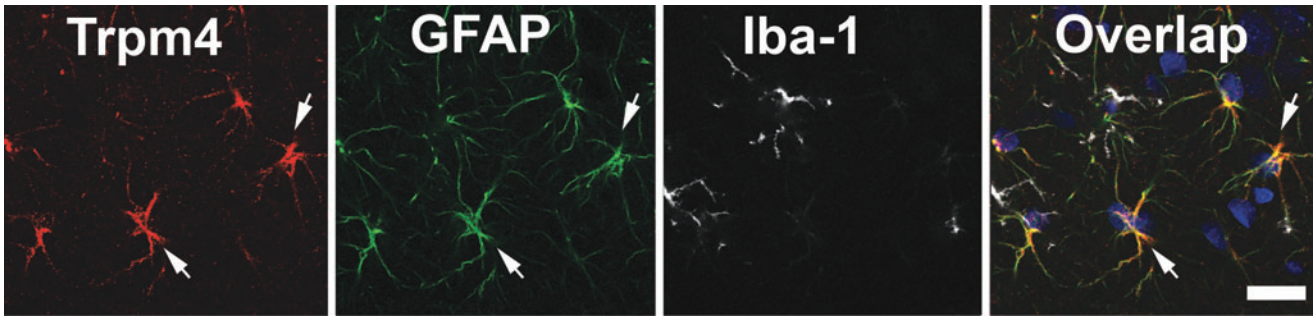

FIG. 2. Representative confocal micrograph from an injured hippocampus triple labeled for transient receptor potential melastatin 4 (Trpm4; red), glial fibrillary acidic protein (GFAP; green), to identify astrocytes, and ionized calcium binding adaptor molecule 1 (Iba-1; white), to identify microglia. Blue in micrographs is 4',6-diamidino-2-phenylindole labeling for nuclei. Cells found to express Trpm4 following diffuse traumatic brain injury also expressed the astrocyte marker, GFAP. Scale bar 20 μm.

injured animals (one-way ANOVA: 8 weeks hippocampal fissure, $F_{1,5}=4.45$, $p=0.089$; 8 weeks gray matter, $F_{1,5}=1.56$, $p=0.267$; 8 weeks whole hippocampus, $F_{1,5}=1.67$, $p=0.253$; Fig. 3F). While there was no effect of time following injury on the number of Trpm4+ astrocytes (two-way ANOVA: hippocampal fissure, $F_{4,28}=1.75$, $p=0.166$; gray matter, $F_{4,28}=0.53$, $p=0.717$), there was a significant effect of injury (hippocampal fissure, $F_{4,28}=33.16$, $p=4\times10^{-6}$; gray matter $F_{4,28}=23.14$, $p=4.7\times10^{-5}$) and there was a significant interaction between injury and time on the number of Trpm4+ astrocytes only within the hippocampal fissure ($F_{4,28}=3.41$, $p=0.022$; gray matter $F_{4,28}=1.66$, $p=0.187$).

To gain an appreciation for the level of Trpm4 expression in individual astrocytes following CFPI, the intensity of Trpm4 labeling in astrocytes within either the hippocampal fissure or the gray matter of the hippocampus were assessed from 6 h to 8 weeks following diffuse TBI using a corrected total cell fluorescence method in which the background corrected total fluorescence of individual cells was assessed as described in the Methods section

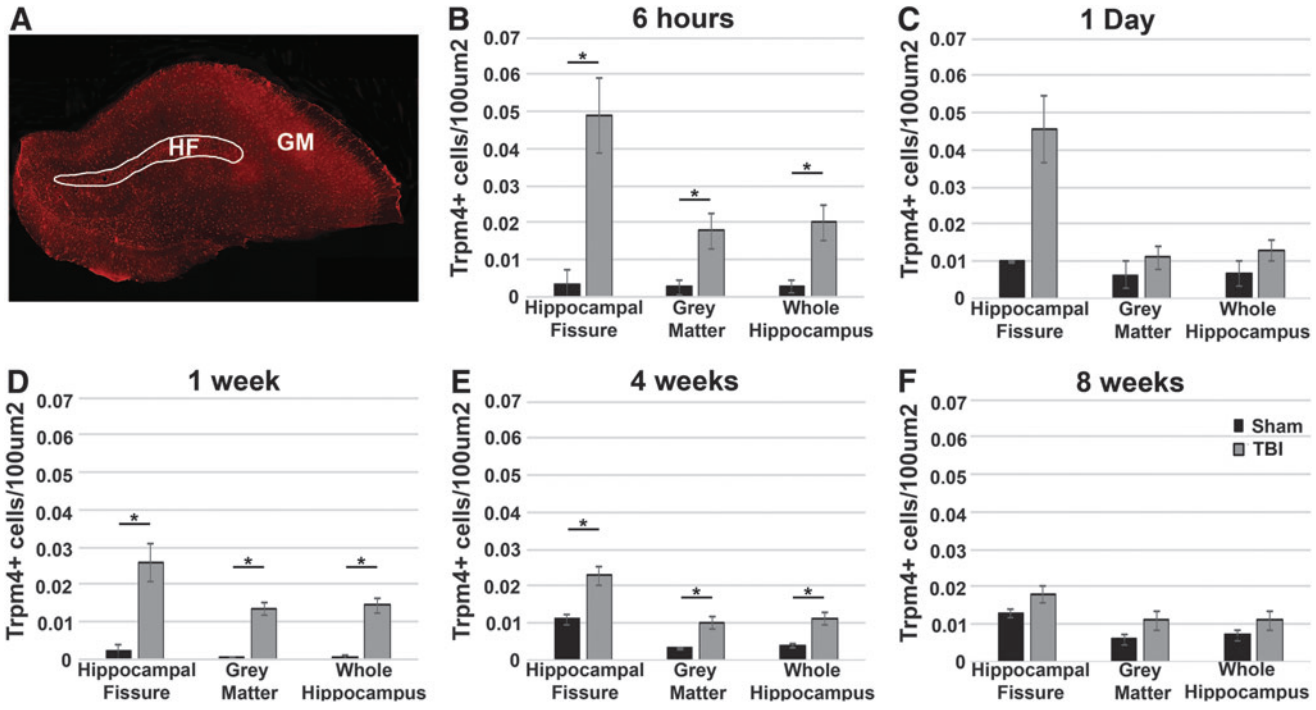

FIG. 3. The number of transient receptor potential melastatin 4 (Trpm4)+ cells in the hippocampus peaks at 6 h post-injury and reduces throughout the first 8 weeks following injury. **(A)** Representative confocal micrograph of the rodent hippocampus 6 h following central fluid percussion injury (CFPI). The indicated region demarcates the hippocampal fissure from the gray matter of the hippocampus. Bar graphs depicting the total number of Trpm4+ cells/100 um^2 of the white matter of the hippocampal fissure, the non-fissure gray matter of the hippocampus, or the entire hippocampus at **(B)** 6 h (sham $n=4$; 6 h traumatic brain injury [TBI] $n=5$), **(C)** 1 day (sham $n=2$; 1 day TBI $n=4$), **(D)** 1 week (sham $n=2$; 1 week TBI $n=6$), **(E)** 4 weeks (sham $n=3$; 4 weeks TBI $n=5$) and **(F)** 8 weeks (sham $n=3$; 8 weeks TBI $n=4$) post-TBI. The trend toward more Trpm4+ cells at 1 day post-injury is nonsignificant; however, the increase in Trpm4+ cells at both 1 week and 4 weeks post-injury is significant. The number of Trpm4+ cells reduces to levels indistinguishable from sham by 8 weeks post-CFPI. Sham represented by black bars and CFPI represented by gray bars. *T*-test against sham for each region of interest at each time-point; error bars represent standard error of the mean. $*p<0.05$.

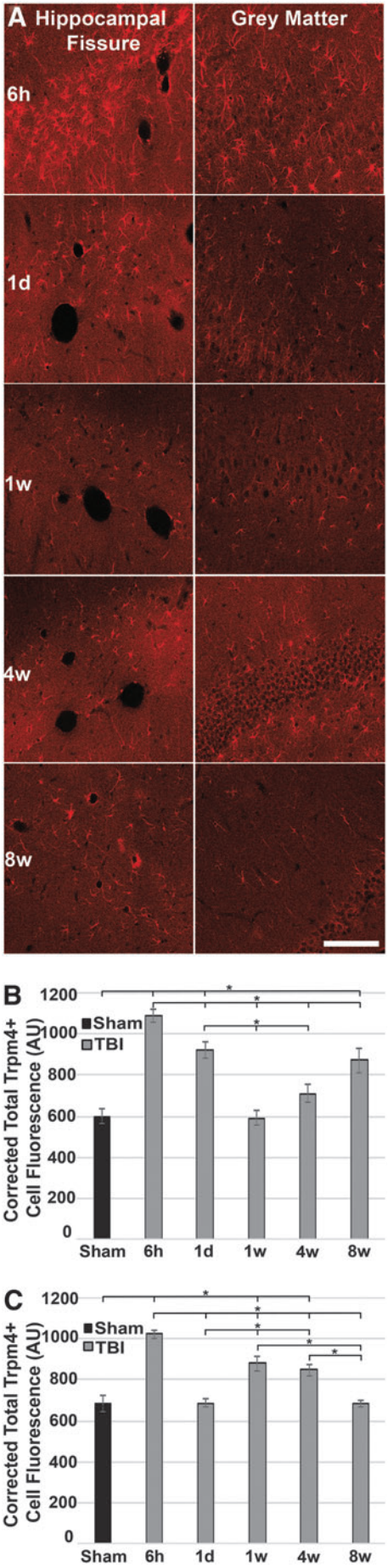

(Fig. 4).[26] As early studies indicate,[9] the cellular intensity of Trpm4 was low in both the hippocampal fissure and the gray matter of the hippocampus in sham-injured rodents. In the white matter of the hippocampal fissure, Trpm4 intensity increased significantly at 6 h post-CFPI, compared with sham and all other time-points (one-way ANOVA: $F_{5,2047} = 20.17$, $p = 1.07 \times 10–19$; Bonferroni *post hoc:* $p = 1.3 \times 10^{-13}$ compared with sham; $p = 0.04$ compared with 1 day; $p = 2.5 \times 10^{-7}$ compared with 1 week; $p = 7.6 \times 10^{-9}$ compared with 4 weeks; $p = 0.012$ compared with 8 weeks; Fig. 4B). Cellular intensity of Trpm4 in the hippocampal fissure also was elevated at 1 day post-CFPI (Bonferroni *post hoc:* $p = 1.5 \times 10^{-4}$ compared with sham; $p = 0.008$ compared with 1 week; $p = 0.045$ compared with 4 weeks; $p = 1.00$ compared with 8 weeks), but decreased to levels indistinguishable from sham at both 1 week and 4 weeks. Interestingly, cellular intensity of Trpm4 was significantly increased above sham levels at 8 weeks in astrocytes within the hippocampal fissure ($p = 0.010$ compared with sham). Simple main effects analysis showed that both injury and time independently affected cellular Trpm4 intensity in the hippocampal fissure (two-way ANOVA: injury. $F_{1,2043} = 7.267$, $p = 0.007$; time. $F_{4,2043} = 3.003$, $p = 0.017$); however, there was no significant interaction between time and injury ($F_{4,2043} = 0.108$, $p = 0.98$).

In the hippocampal gray matter, intensity of Trpm4 in individual astrocytes also was significantly increased at 6 h post-CFPI, compared with sham levels and all other time-points (one-way ANOVA: $F_{5,5870} = 41.43$, $p = 4.7 \times 10^{-42}$; Bonferroni *post hoc:* $p = 4.8 \times 10^{-10}$ compared with sham; $p = 2.9 \times 10^{-25}$ compared with 1 day; $p = 0.001$ compared with 1 week; $p = 4.6 \times 10^{-7}$ compared with 4 weeks; $p = 4.2 \times 10^{-31}$ compared with 8 weeks; Fig. 4C). At 1 day post-injury, however, astrocytic Trpm4 intensity within individual cells in the gray matter of the hippocampus was comparable to sham levels. Trpm4 astrocytic intensity was increased above sham and 1 day post-TBI levels at both 1 week (Bonferroni *post hoc:* $p = 0.010$ compared with sham; $p = 4.1 \times 10^{-5}$ compared with 1 day; $p = 7.0 \times 10^{-6}$ compared with 8 weeks) and 4 weeks (Bonferroni *post hoc:* $p = 0.037$ compared with sham; $p = 1.7 \times 10^{-4}$ compared with 1 day; $p = 2.4 \times 10^{-5}$ compared with 8 weeks), then returned to levels comparable to sham at 8 weeks post-CFPI. There was a significant interaction between injury and time on the

FIG. 4. The cellular expression of transient receptor potential melastatin 4 (Trpm4) peaks at 6 h post-injury and occurs in waves. **(A)** Representative confocal micrographs of the hippocampal fissure and gray matter of the hippocampus at 6 h, 1 day, 1 week, 4 weeks, and 8 weeks post–central fluid percussion injury (CFPI). **(B)** Bar graph depicting the average background corrected total cell fluorescence of individual Trpm4+ cells in the hippocampal fissure of sham-injured rats ($n = 227$ cells from four animals), or rats subject to CFPI and killed at 6 h ($n = 934$ cells from four animals), 1 day ($n = 322$ cells from four animals), 1 week ($n = 104$ cells from four animals), 4 weeks ($n = 250$ cells from four animals) or 8 weeks ($n = 216$ cells from four animals). **(C)** Bar graph depicting the average corrected total cell fluorescence of Trpm4+ cells in the hippocampal gray matter of sham-injured rats ($n = 264$ cells from four animals), or rats subject to CFPI and killed at 6 h ($n = 2095$ cells from four animals), 1 day ($n = 870$ cells from four animals), 1 week ($n = 608$ cells from four animals), 4 weeks ($n = 888$ cells from four animals) or 8 weeks ($n = 1151$ cells from four animals). Sham represented by black bars and CFPI represented by gray bars. Analysis of variance with Bonferroni *post hoc* test; error bars represent standard error of the mean. $*p < 0.05$. Scale bar 100 μm.

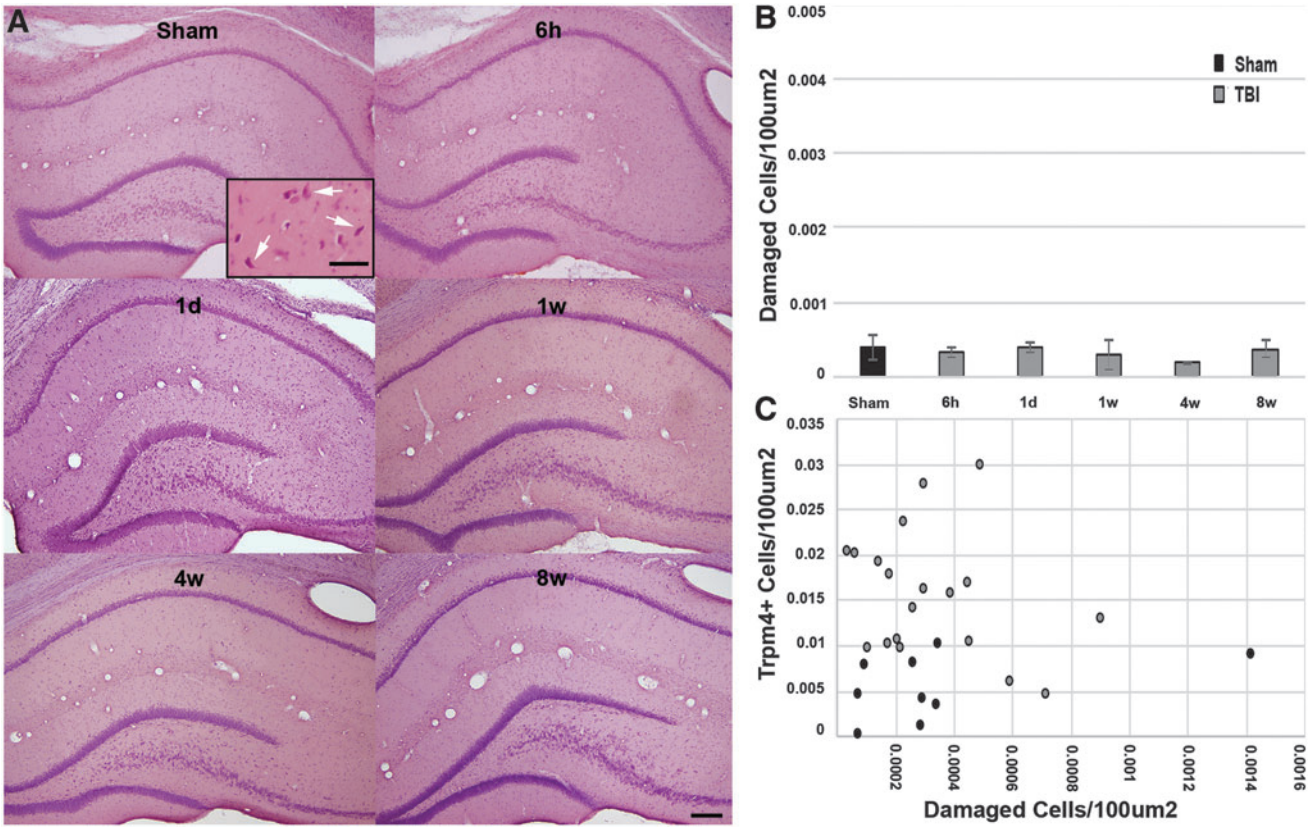

FIG. 5. Transient receptor potential melastatin 4 (Trpm4) expression is not correlated to cell damage/death following diffuse moderate traumatic brain injury (TBI). **(A)** Representative light micrographs of the hippocampus from sham-injured or TBI animals at 6 h, 1 day, 1 week, 4 weeks, and 8 weeks. Inset depicts damaged cells demonstrating pyknotic nuclei and eosinophilic cytoplasm from a positive control (arrows). **(B)** Bar graph depicting the average number of damaged or dying cells/100 um^2 in the entire hippocampus. Note that at no time-point do the numbers of damaged/dying cells increase above sham levels. **(C)** Scatterplot illustrating the lack of correlation between average number of Trpm4+ cells and average number of damaged/dying cells in the entire hippocampus. Each point represents an individual animal sustaining either sham injury or central fluid percussion injury (CFPI). Sham $n=7$, 6 h $n=5$, 1 day $n=5$, 1 week $n=4$, 4 weeks $n=4$, 8 weeks $n=4$. Sham represented by black bars and CFPI represented by gray bars. Analysis of variance with Bonferroni *post hoc* test; error bars represent standard error of the mean scale bar (A) 200 μm; inset 50 μm.

intensity/expression of Trpm4 in individual cells of hippocampal gray matter (two-way ANOVA: $F_{4,5866}=4.48$, $p=0.001$).

Expression of Trpm4 does not precipitate cellular damage, but is associated with astrocyte swelling following diffuse traumatic brain injury

Since expression of the Trpm4 channel, with or without Sur1 association, is associated with cell death in hemorrhagic contusion expansion,[19,23,28–30] we evaluated the number of damaged/dead cells throughout the entire hippocampus 6 h to 8 weeks following CFPI. To determine damaged/dead cells, tissue was labeled with H&E. Any cell exhibiting a heterochromatic nucleus and eosinophilic cytoplasm was identified as damaged (Fig. 5).[27] No overt cell damage or death was observed in the hippocampus at any time-point (one way ANOVA: $F_{5,23}=0.293$, $p=0.912$; Fig. 5A, 5B). There also was no detectable correlation between the number of Trpm4+ astrocytes and number of damaged cells/100 μm^2 in the hippocampus (Spearmen's rho = 0.038, $R^2=0.005$, $p=0.85$; Fig. 5C).

Since the evaluation of damaged/dead cells was not specific to astrocytes, concomitant ultrastructural analysis was performed to further investigate the potential for cellular damage in the hippocampal astrocyte population. The most chronic time-point assessed in which Trpm4 was highly expressed by individual astrocytes in the hippocampal gray matter was 4 weeks post-CFPI (Fig. 4C); therefore, astrocytes within the hippocampal gray matter at 4weeks post-injury were assessed. None of the Trpm4+ astrocytes demonstrated ultrastructural characteristics of damaged or dying cells, including mitochondrial change, vesicular swelling, pyknosis or peripheral lucent zones (Fig. 6).

To explore the potential association between Trpm4 cellular intensity/expression levels and astrocyte swelling, we assessed the potential correlation between cell size and the average mean gray value for individual Trpm4+ astrocytes in confocal micrographs. There were no significant correlations between astrocyte size and Trpm4 intensity following sham injury or in the hippocampal gray matter at 1 day or the hippocampal fissure 1 week post-CFPI (sham hippocampal fissure Spearman's rho = 0.08, $p=0.19$, $n=227$; sham Spearman's rho = 0.02, $p=0.812$, $n=264$; 1 day hippocampal gray matter Spearman's rho = 0.03, $p=0.468$, $n=870$ cells; 1 week hippocampal fissure Spearman's rho = 0.07, $p=0.475$, $n=104$ cells). However, this correlation was observed in most post-injury time-points in both the hippocampal fissure and the gray matter of the hippocampus (6 h hippocampal fissure Spearman's rho = 0.21, $p=9.5\times10^{-11}$, $n=934$ cells; 6 h hippocampal gray matter Spearman's rho = 0.114, $p=1.6\times10^{-7}$, $n=2095$ cells; 1 day hippocampal

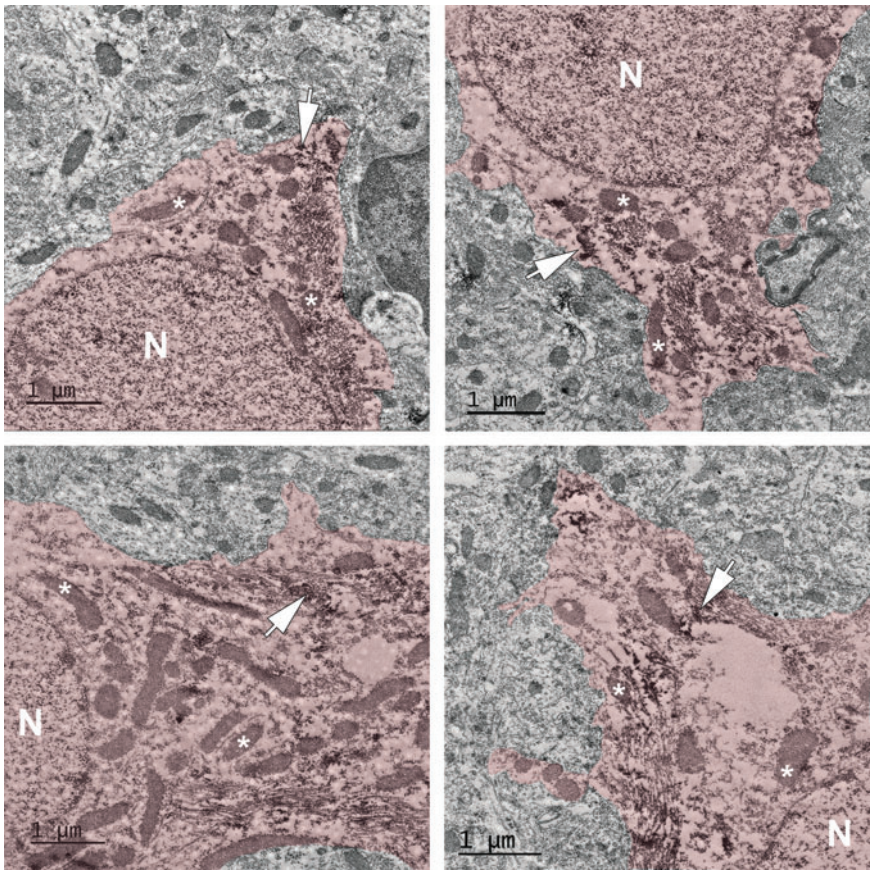

FIG. 6. Transient receptor potential melastatin 4 (Trpm4)+ astrocytes do not display signs of overt ultrastructural damage. Representative electron micrographs of astrocytes from the hippocampal gray matter 4 weeks post–central fluid percussion injury labeled against Trpm4 (red pseudo colored cells). Astrocytes were identified based on their unique ultrastructural characteristics; primarily the combination of euchromatic nuclei (N) and electron lucent cytoplasm. Arrows indicate immunoreactivity against Trpm4 visualized with electron dense diaminobenzidine reaction product. Note that the Trpm4+ astrocytes do not demonstrate any ultrastructural indicators of cellular damage or eminent death and have structurally normal mitochondria (*). Also note the lack of structural pathology in the surrounding parenchyma. Scale bar 1 μm.

fissure Spearman's rho = 0.21, $p = 1.3 \times 10^{-4}$, $n = 322$ cells; 1 week hippocampal gray matter Spearman's rho = 0.20, $p = 5.7 \times 10^{-7}$, $n = 2095$ cells; 4 weeks hippocampal fissure Spearman's rho = 0.22, $p = 1.1 \times 10^{-12}$, $n = 250$ cells; 8 weeks hippocampal fissure Spearman's rho = 0.22, $p = 0.001$, $n = 216$ cells; 8 weeks hippocampal gray matter Spearman's rho = 0.11, $p = 1.9 \times 10^{-4}$, $n = 1151$ cells). The largest effect size was observed between astrocyte size and the intensity of Trpm4+ cells in the gray matter of the hippocampus at 4 weeks post-CFPI (Spearman's rho = 0.238, $p = 8.25 \times 10^{-18}$, $n = 888$ cells); therefore, subsequent ultrastructural evaluations of soma size were done at 4 weeks post-injury in the gray matter of the hippocampus.

To evaluate the strength of our confocal cellular size analysis, we performed quantitative ultrastructural assessments of the somal cytoplasmic area of Trpm4+ and Trpm4- astrocytes within the gray matter of the hippocampus 4 weeks post-CFPI. This assessment revealed Trpm4+ astrocytes had nearly double the soma size, compared with Trpm4- astrocytes (one-way ANOVA: $F_{1,165} = 59.19$, $p = 1.2 \times 10^{-12}$; Fig. 7).

Discussion

In the current study, we evaluated the expression of Trpm4 over an 8-week time course following diffuse TBI using the CFPI model in adult male rats. We found that Trpm4 was expressed by astrocytes within the hippocampus. Trpm4, as a component of the Sur1–Trpm4 channel, has been implicated in the progression of cytotoxic edema and oncotic cell death leading to hemorrhagic contusion expansion following a variety of focal brain injuries.[13–17] Correlated cell death within the hippocampus, however, was not observed at any time-point following CFPI, indicating that oncosis did not ensue following diffuse TBI. Additionally, we did not observe any overt ultrastructural change that would indicate that Trpm4+ astrocytes were at early stages of cellular degeneration. Interestingly, sub-acute astrocytic expression of Trpm4 also was observed in human tissue out to 31 days following a cerebral infarct,[31] indicating that Trpm4 expression, at least in astrocytes, may not always result in acute cell death.

Confocal and ultrastructural evaluations of Trpm4+ astrocytes did, however, show a significant increase in soma size correlated with Trpm4 expression following CFPI. Astrocyte size was found to correlate significantly with Trpm4 intensity/expression in individual cells in both regions of the hippocampus at all time-points in which Trpm4 cellular expression was elevated. Trpm4+ astrocytes were also found to have nearly double the average soma size, compared with Trpm4- astrocytes. This indicates that expression of Trpm4 in astrocytes following CFPI is associated with astrocyte swelling without precipitating oncotic cell death.

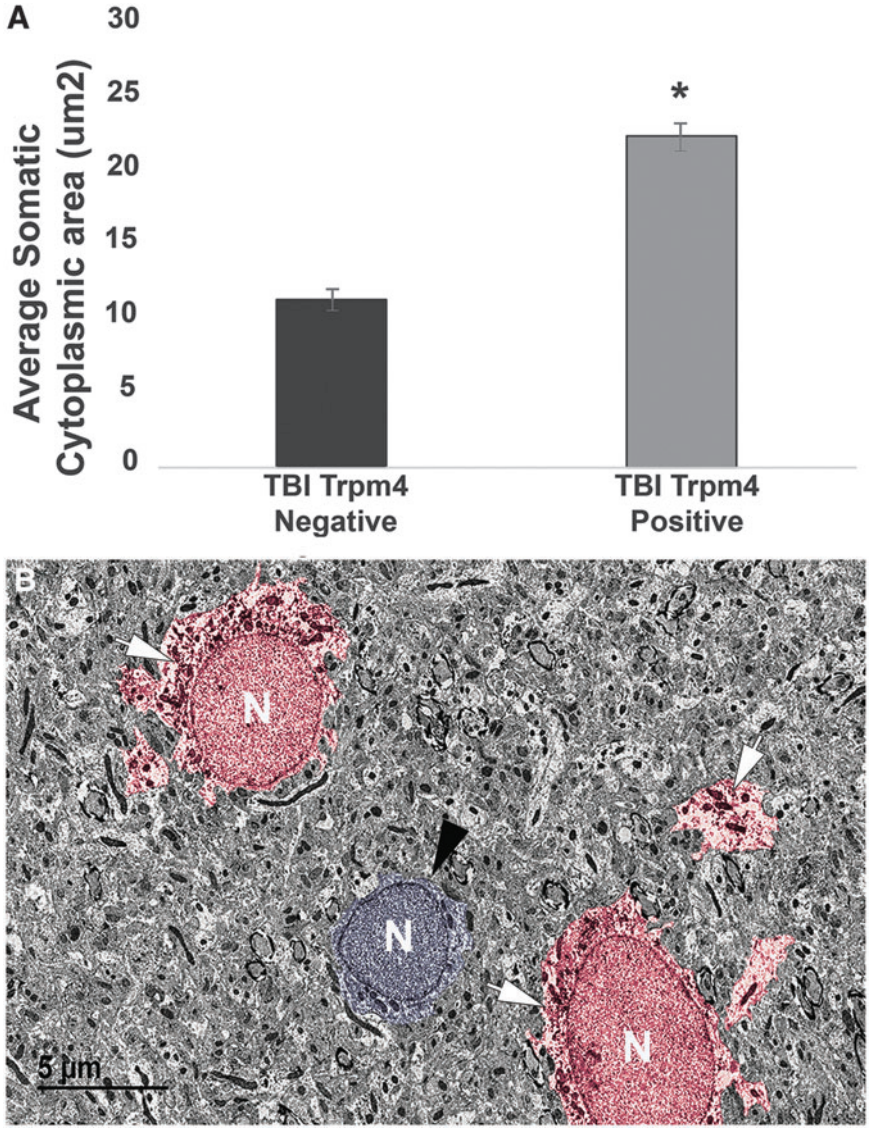

FIG. 7. Astrocytes expressing transient receptor potential melastatin 4 (Trpm4) have a greater somatic cytoplasmic area indicating cellular swelling. **(A)** Bar graph depicting the average area of the somatic cytoplasm surrounding the nucleus. Trpm4 expression nearly doubled the astrocyte cytoplasmic area, compared with Trpm4- astrocytes. **(B)** Representative electron micrograph of astrocytes from the hippocampal gray matter 4 weeks post–central fluid percussion injury labeled against Trpm4 (white arrows; red pseudo color). The arrows indicate immunoreactivity against Trpm4. The astrocyte in the middle of the electron micrograph (black arrow head; blue pseudo color) is a Trpm4- astrocyte located between two Trpm4+ astrocytes. N indicates the nucleus of each cell. Traumatic brain injury (TBI), three animals Trpm4- $n=57$ cells, Trpm4+ $n=110$ cells. Analysis of variance; error bars represent standard error of the mean. $^*p<0.05$. Scale bar 5 μm.

In the non-injured brain, astrocytes modulate the movement of ions[32,33]—and thus water—between the brain parenchyma, the astrocytic cytoplasm, and the blood. This modulation involves the passive diffusion of water through the aquaporin 4 (AQP4) channel in astrocytic endfeet, which make up the outermost layer of the blood–brain barrier.[34,35] This system neutralizes osmotic gradients generated by ion transporters. It was recently found that AQP4 co-associates with the Sur1–Trpm4 channel and that this co-association modulates astrocyte swelling.[36] In the case of Trpm4-mediated cytotoxic edema during hemorrhagic contusion expansion, it is proposed that an influx of ions through the Sur1–Trpm4 channel generates an osmotic gradient between the brain and the blood that is high enough to precipitate Na+ movement from the blood to the brain parenchyma causing vasogenic edema in which water also moves out of the blood and into the brain, ultimately leading to oncotic cell death.[35] While ion and water movement precipitating astrocyte swelling are likely in the case of diffuse TBI, the final stage resulting in cell death due to cell swelling does not appear to occur, as evidenced by the lack of damaged cells throughout the hippocampus and the ultrastructural normality of Trpm4+ astrocytes.

Recent studies indicate that short nucleotide polymorphisms (SNPs) of the Sur1 component of the Sur1–Trpm4 channel are correlated with cerebral edema.[37] These data appear to support a potential neutral or even ameliorative role for Trpm4 or Sur1-Trpm4, with major SNP alleles being either non-correlated or protective in terms of cerebral edema formation.[37] Additionally,

previous studies show that while there is a trend to higher brain water content following CFPI, there is no significant edema resulting from the CFPI model.[38] The characteristics of ion movement in the Trpm4+ astrocytes following diffuse CFPI, and the osmotic gradients generated thereby, are likely to be less than that seen in focal damage, but require further investigation.

Astrocyte size was directly correlated with the intensity/expression level of Trpm4, suggesting a potential relationship between the degree of Trpm4 expression and astrocyte cell swelling. Trpm4 expression peaked at 6 h following injury, both in terms of total number of Trpm4+ astrocytes in the hippocampus, as well as the cellular intensity of Trpm4 labeling. While the number of Trpm4+ astrocytes decreased gradually from 6 h to 8weeks following injury, the intensity of Trpm4 in individual astrocytes changed over the time course, with temporal properties differing between the white and gray matter of the hippocampus. Interestingly, the region-specific time-points in which Trpm4 expression was lowest following CFPI (1 week for the hippocampal fissure and 1 day for the hippocampal gray matter) were the same region-specific time-points in which correlation between astrocyte size and Trpm4 intensity level were not observed. To our knowledge this is the first study to report variations in Trpm4 expression levels between astrocytes within the gray and white matter of the hippocampus. This dissimilarity in Trpm4 intensity/expression could reflect variations in astrocyte subtype within the gray and white matter of the hippocampus.

Heterogeneity of astrocytes in various regions of the brain have been well-characterized.[39–41] Specifically, astrocytes within the hippocampus fall into either glutamate transporter expressing (GluT) or AMPA-type glutamate receptor expressing (GluR) subtypes that differ morphologically, electrophysiologically, and molecularly.[42] Interestingly, the GluR hippocampal astrocytes have no discernable gap junctional coupling, whereas the GluT astrocytes have substantial coupling,[43] which could protect individual astrocytes from oncosis due to localized edema, as cellular challenges could be shared with neighboring astrocytes. The GluR and GluT astrocyte subtypes are diffusely dispersed throughout the hippocampal gray matter[43]; however, the predominant astrocyte subtype within the hippocampal fissure remains to be determined. Future explorations of Trpm4 expression in GluR and GluT hippocampal astrocytes normally and following injury, might further inform the role of astrocytic swelling in the face of diffuse brain injury.

Ultimately, these studies demonstrate that while Trpm4 expression is associated with astrocyte swelling, it does not precipitate cell death following diffuse TBI. Further, diffuse Trpm4 expression is region-specific. These studies provide a foundation for further exploration into Trpm4 and potential astrocyte swelling following diffuse TBI, which could provide guidance for the treatment of edema following brain injury.

Acknowledgments

The authors would like to thank Dr. Mark Simard, Dr. Nikki Miller Ferguson, and Dr. John Povlishock for stimulating scientific discussion, and Dr. Mark Simard for the kind gift of the rabbit anti-Sur1 antibody. We would also like to thank Sue Walker, Judy Williamson, and Lynn Davis for instrumental technical and regulatory assistance. This work was supported in part by National Institute of Neurological Disorders and Stroke (NINDS) grants 1R01NS096143 and the Commonwealth fund. Microscopy was performed at the Virginia Commonwealth University Department of Anatomy and Neurobiology Microscopy Facility, supported in part by funding from NIH-NINDS Center core grant 5P30NS047463.

Author Disclosure Statement

No competing financial interests exist.

References

1. Faul, M., Xu, L, Wald, MM, and Coronado, V.G. (2010). *Traumatic Brain Injury in the United States: Emergency Department Visits, Hospitalizations and Deaths 2002–2006.* Centers for Disease Control and Prevention, National Center for Injury Prevention and Control: Atlanta, GA, pps. 2–70.
2. Langlois, J.A., Rutland-Brown, W., and Wald, M.M. (2006). The epidemiology and impact of traumatic brain injury: a brief overview. J. Head Trauma Rehabil. 21, 375–378.
3. Cernak, I., Vink, R., Zapple, D.N., Cruz, M.I., and Ahmed, F. (2004). The pathobiology of moderate diffuse traumatic brain injury as identified using a new experimental model of injury in rats. Neurobiol. Dis. 17, 29–43.
4. Lafrenaye, A.D., Krahe, T.E., and Povlishock, J.T. (2014). Moderately elevated intracranial pressure after diffuse traumatic brain injury is associated with exacerbated neuronal pathology and behavioral morbidity in the rat. J. Cereb. Blood Flow Metab. 34, 1628–1636.
5. Povlishock, J.T. and Christman, C.W. (1995). The pathobiology of traumatically induced axonal injury in animals and humans: a review of current thoughts. J. Neurotrauma 12, 555–564.
6. Erb, D. and Povlishock, J. (1991). Neuroplasticity following traumatic brain injury: a study of GABAergic terminal loss and recovery in the cat dorsal lateral vestibular nucleus. Exp. Brain Res. 83, 253–267.
7. Kasahara, M., Menon, D., Salmond, C., Outtrim, J., Tavares, J., Carpenter, T., Pickard, J., Sahakian, B., and Stamatakis, E. (2010). Altered functional connectivity in the motor network after traumatic brain injury. Neurology 75, 168–176.
8. Ramsey, I.S., Delling, M., and Clapham, D.E. (2006). An introduction to TRP channels. Annu. Rev. Physiol. 68, 619–647.
9. Launay, P., Fleig, A., Perraud, A.L., Scharenberg, A.M., Penner, R., and Kinet, J.P. (2002). TRPM4 is a Ca2+-activated nonselective cation channel mediating cell membrane depolarization. Cell 109, 397–407.
10. Guinamard, R., Demion, M., and Launay, P. (2010). Physiological roles of the TRPM4 channel extracted from background currents. Physiology 25, 155–164.
11. Nilius, B., Prenen, J., Voets, T., and Droogmans, G. (2004). Intracellular nucleotides and polyamines inhibit the Ca2+-activated cation channel TRPM4b. Pflugers Arch. 448, 70–75.
12. Nilius, B., Prenen, J., Tang, J., Wang, C., and Owsianik, G. (2005). Regulation of the Ca2+ sensitivity of the nonselective cation channel TRPM4. J. Biol. Chem. 280, 6423–6433.
13. Gerzanich, V., Woo, K.S., Vennekens, R., Tsymbalyuk, O., Ivanova, S., Ivanov, A., Geng, Z., Chen, Z., Nilius, B., Flockerzi, V., Freichel, M., and Simard, M.J. (2009). De novo expression of Trpm4 initiates secondary hemorrhage in spinal cord injury. Nat. Med. 15, 185–191.
14. Woo, S., Kwon, M., Ivanov, A., Gerzanich, V., and Simard, M.J. (2013). The sulfonylurea receptor 1 (Sur1)-transient receptor potential melastatin 4 (Trpm4) channel*. J. Biol. Chem. 288, 3655–3667.
15. Simard, J.M., Woo, S.K., Schwartzbauer, G.T., and Gerzanich, V. (2012). Sulfonylurea receptor 1 in central nervous system injury: a focused review. J. Cereb. Blood Flow Metab. 32, 1699–1717.
16. Simard, M.J., Woo, K.S., and Gerzanich, V. (2012). Transient receptor potential melastatin 4 and cell death. Pflügers Arch. 464, 573–582.
17. Martínez-Valverde, T., Vidal-Jorge, M., Martínez-Saez, E., Castro, L., Arikan, F., Cordero, E., R doi, A., Poca, M.A.A., Simard, J.M., and Sahuquillo, J. (2015). Sulfonylurea receptor 1 in humans with post-traumatic brain contusions. J. Neurotrauma 32, 1478–1487.
18. Boggs, D.H., Simard, J.M., Steven, A., and Mehta, M.P. (2014). Potential of glyburide to reduce intracerebral edema in brain metastases. Expert. Rev. Neurother. 14, 379–388.

19. Simard, J.M., Kahle, K.T., and Gerzanich, V. (2010). Molecular mechanisms of microvascular failure in central nervous system injury–synergistic roles of NKCC1 and SUR1/TRPM4. J. Neurosurg. 113, 622–629.
20. Simard, M.J., Tsymbalyuk, O., Keledjian, K., Ivanov, A., Ivanova, S., and Gerzanich, V. (2012). Comparative effects of glibenclamide and riluzole in a rat model of severe cervical spinal cord injury. Exp. Neurol. 233, 566–574.
21. Kurland, D.B., Tosun, C., Pampori, A., Karimy, J.K., Caffes, N.M., Gerzanich, V., and Simard, M.J. (2013). Glibenclamide for the treatment of acute CNS injury. Pharmaceuticals 6, 1287–1303.
22. Simard, M.J., Tsymbalyuk, O., Ivanov, A., Ivanova, S., Bhatta, S., Geng, Z., Woo, K.S., and Gerzanich, V. (2007). Endothelial sulfonylurea receptor 1 regulated NCCa-ATP channels mediate progressive hemorrhagic necrosis following spinal cord injury. J. Clin. Invest. 117, 2105–2113.
23. Popovich, P.G., Lemeshow, S., Gensel, J.C., and Tovar, A.C. (2012). Independent evaluation of the effects of glibenclamide on reducing progressive hemorrhagic necrosis after cervical spinal cord injury. Exp. Neurol. 233, 615–622.
24. Simard, M.J., Chen, M., Tarasov, K.V., Bhatta, S., Ivanova, S., Melnitchenko, L., Tsymbalyuk, N., West, A.G., and Gerzanich, V. (2006). Newly expressed SUR1-regulated NCCa-ATP channel mediates cerebral edema after ischemic stroke. Nat. Med. 12, 433–440.
25. Dixon, C., Lyeth, B., Povlishock, J., Findling, R., Hamm, R., Marmarou, A., Young, H., and Hayes, R. (1987). A fluid percussion model of experimental brain injury in the rat. J. Neurosurg. 67, 110–119.
26. ScienceTechBlog. (2012). Measuring Cell Fluorescence Using ImageJ. Available at: https://sciencetechblog.files.wordpress.com/2011/05/measuring-cell-fluorescence-using-imagej.pdf. Accessed March 29, 2018.
27. Lafrenaye, A., McGinn, M., and Povlishock, J. (2012). Increased intracranial pressure after diffuse traumatic brain injury exacerbates neuronal somatic membrane poration but not axonal injury: evidence for primary intracranial pressure-induced neuronal perturbation. J. Cereb. Blood Flow Metab. 32, 1919–1932.
28. Sala-Rabanal, M., Wang, S., and Nichols, C. (2012). On potential interactions between non-selective cation channel TRPM4 and sulfonylurea receptor SUR1. J. Biol. Chem. 287, 8746–8756.
29. Jiang, B., Li, L., Chen, Q., Tao, Y., Yang, L., Zhang, B., Zhang, J.H., Feng, H., Chen, Z., Tang, J., and Zhu, G. (2017). Role of glibenclamide in brain injury after intracerebral hemorrhage. Transl. Stroke Res. 8, 183–193.
30. Hayman, E.G., Wessell, A., Gerzanich, V., Sheth, K.N., and Simard, J.M. (2017). Mechanisms of global cerebral edema formation in aneurysmal subarachnoid hemorrhage. Neurocrit. Care 26, 301–310.
31. Mehta, R.I., Tosun, C., Ivanova, S., Tsymbalyuk, N., Famakin, B.M., Kwon, M.S., Castellani, R.J., Gerzanich, V., and Simard, J.M. (2015). Sur1-Trpm4 cation channel expression in human cerebral infarcts. J. Neuropathol. Exp. Neurol. 74, 835–849.
32. Somjen, G.G. (2002). Ion regulation in the brain: implications for pathophysiology. Neuroscientist 8, 254–267.
33. Chen, Y. and Swanson, R. (2003). Astrocytes and brain injury. J. Cereb. Blood Flow Metab. 23, 137–149.
34. Papadopoulos, M. and Verkman, A. (2013). Aquaporin water channels in the nervous system. Nat. Rev. Neurosci. 14, 265–277.
35. Stokum, JA, Kurland, DB, Gerzanich, V, and Simard, JM. (2015). Mechanisms of astrocyte-mediated cerebral edema. Neurochem. Res. 40, 317–328.
36. Stokum, J.A., Kwon, M.S., Woo, S.K., Tsymbalyuk, O., Vennekens, R., Gerzanich, V., and Simard, J.M. (2018). SUR1-TRPM4 and AQP4 form a heteromultimeric complex that amplifies ion/water osmotic coupling and drives astrocyte swelling. Glia 66, 108–125.
37. Jha, R.M., Puccio, A.M., Okonkwo, D.O., Zusman, B.E., Park, S.-Y.Y., Wallisch, J., Empey, P.E., Shutter, L.A., Clark, R.S., Kochanek, P.M., and Conley, Y.P. (2017). ABCC8 single nucleotide polymorphisms are associated with cerebral edema in severe TBI. Neurocrit. Care 26, 213–224.
38. Fenn, A.M., Skendelas, J.P., Moussa, D.N., Muccigrosso, M.M., Popovich, P.G., Lifshitz, J., Eiferman, D.S., and Godbout, J.P. (2015). Methylene blue attenuates traumatic brain injury-associated neuroinflammation and acute depressive-like behavior in mice. J. Neurotrauma 32, 127–138.
39. Andriezen, L.W. (1893). The neuroglia elements in the human brain. BMJ 2, 227.
40. Zhang, Y. and Barres, B. (2010). Astrocyte heterogeneity: an underappreciated topic in neurobiology. Curr. Opin. Neurobiol. 20, 588–594.
41. Oberheim, N., Goldman, S., and Nedergaard, M. (2012). Heterogeneity of astrocytic form and function. Methods Mol. Biol. 814, 23–45.
42. Matthias, K., Kirchhoff, F., Seifert, G., Hüttmann, K., Matyash, M., Kettenmann, H., and Steinhäuser, C. (2003). Segregated expression of AMPA-type glutamate receptors and glutamate transporters defines distinct astrocyte populations in the mouse hippocampus. J. Neurosci. 23, 1750–1758.
43. Wallraff, A., Odermatt, B., Willecke, K., and Steinhäuser, C. (2004). Distinct types of astroglial cells in the hippocampus differ in gap junction coupling. Glia 48, 36–43.

Address correspondence to:
Audrey D. Lafrenaye, PhD
Department of Anatomy and Neurobiology
Virginia Commonwealth University Medical Center
PO Box 980709
Richmond, VA 23298

E-mail: audrey.lafrenaye@vcuhealth.org